Adsorption and Thermal Conversion of 2-Iodoethanol on Ni(100) Surfaces: Hydroxyalkyls and Oxametallacycles as Key Intermediates during the Catalytic Oxidation of Hydrocarbons

By Qing Zhao and Francisco Zaera*

Department of Chemistry, University of California, Riverside, Riverside, California 92521

Received: April 14, 2003; In Final Form: June 17, 2003

The adsorption and thermal reactions of 2-iodoethanol on clean Ni(100) single-crystal surfaces were studied by temperature-programmed desorption (TPD) and X-ray photoelectron spectroscopy (XPS). 2-Iodoethanol was chosen as a precursor for the preparation of 2-hydroxyethyl and oxametallacycle surface species, potential intermediates in hydrocarbon catalytic oxidations. It was found that 2-iodoethanol adsorbs molecularly at 100 K, in two configurations involving either just the iodine atom or both iodine and hydroxyl ends of the molecule. A complex chemical behavior starts around 140 K with the production of small amounts of ethylene and water, most likely via the concerted decomposition or disproportionation of the adsorbed molecular species. The bulk of the 2-iodoethanol decomposes at about 150 K via an initial carbon−iodine scission to form $-O(H)CH_2CH_2-$ (∼80%) and 2-hydroxyethyl (∼20%) intermediates. Two competing reactions are involved with the subsequent conversion of the 2-hydroxyethyl species around 160 K, a reductive elimination with surface hydrogen to yield ethanol, and a β−H elimination to surface vinyl alcohol. The $-O(H)CH_2CH_2-$, on the other hand, dehydrogenates to a $-OCH_2CH_2-$ oxametallacycle species about the same temperature. Both 2-hydroxyethyl and the oxametallacycle species tautomerize to acetaldehyde, around 210 K and above 250 K, respectively, and some of that acetaldehyde desorbs, whereas the rest decomposes to hydrogen and carbon monoxide. The implications of this chemistry to catalysis are discussed.

1. Introduction

Heterogeneous catalysis is at the center of most industrial processes, accounting for about a quarter of the world's gross domestic product.[1] The original goal in using catalysts for the production and processing of chemicals was to increase the rate of the chemical reactions involved, but as more complex catalytic processes were developed, the emphasis shifted toward improving their selectivity.[2] A reaction that is highly selective toward the desired product(s) is bound to consume less reactants, minimize the need for expensive and difficult separation processes, and create less polluting byproducts. A molecular-level control of the selectivity of catalysts is arguably the single most important challenge in this field for the future.[3] The problem of achieving acceptable selectivities in industrial processes is particularly acute in hydrocarbon oxidation, because there the most thermodynamically favorable reactions usually lead to the formation of undesirable products such as carbon oxides and water.[4−6] Selectivity toward useful partial oxidation compounds can only be accomplished via kinetic control, but that requires a good understanding of the surface reaction mechanisms.[3,7] As part of our effort to enhance the basic knowledge on hydrocarbon catalytic oxidation reactions,[8−13] here we report on the surface chemistry of 2-iodoethanol on Ni(100) single-crystal surfaces.

Oxametallacycle complexes have been proposed as crucial intermediates in a variety of homogeneously catalyzed reactions, including selective alkane and olefin oxidation, and carbonylation and decarbonylation chemistry.[14,15] Analogous surface oxametallacycles have also been invoked to explain many heterogeneously catalytic reactions. In surface science, the formation of oxametallacycles has been proposed for the ring opening of epoxides that take place on a number of group VIII metal surfaces, including Pd(110), Pd(111), and Rh(111).[16−18] Extensive work on the epoxidation of olefins by silver catalysts also suggests the formation of surface oxametallacycle intermediates,[19−21] although direct evidence for that mechanism is still unavailable.

Our interest in oxametallacycles relates to an issue of selectivity between dehydrogenation and dehydration products during the catalytic oxidation of alkanes and alcohols. It is known that, in general, basic oxides such as magnesia and calcium oxide promote the dehydrogenation of alcohols to aldehydes or ketones, whereas acidic oxides such as γ-alumina promote their dehydration to olefins instead.[22] Alcohol dehydrogenation is believed to occur via β-hydride elimination from the surface alkoxides formed by an initial facile hydroxyl hydrogen removal step.[8,23] Alcohol dehydration, on the other hand, often involves acid−base chemistry similar to that known in homogeneous organic reactions.[24,25] There is, however, a chance to induce alcohol dehydration on nonacidic solids if alkoxides can be forced to undergo γ-hydride elimination and form surface oxametallacycle intermediates. Those intermediates can then presumably decompose by oxygen elimination to yield the corresponding olefin. This report focuses on testing the latter hypothesis.

2-Iodoethanol was chosen as precursor for the preparation of oxametallacycle surface intermediates based on the reports by us and others on the extensive and successful use of halohydrocarbons to prepare a wide range of surface intermediates, including alkyls,[26−28] carbenes,[29−33] vinyls,[34,35] allyls,[36−39]

* To whom correspondence should be addressed.

10.1021/jp035004f CCC: $25.00
Published on Web 07/23/2003

and metallacycles.[33,40−44] The premise behind the use of those precursors is that carbon−halogen bonds, carbon−iodine bonds in particular, are weak and easy to activate on adsorbed species and that the surface halide byproduct of that reaction does not significantly affect the subsequent chemistry of the resulting adsorbed hydrocarbon moieties.[27,45−48] However, the same about the ease of activation can be said for the O−H bond in alcohols, hence their propensity to form alkoxide groups upon adsorption on metals.[5,49,50] This provides an additional level of complexity when using halo alcohols in the preparation of surface intermediates. Nevertheless, convincing evidence has already been provided for the transformation of 2-iodoethanol to oxametallacycle surface species on silver surfaces.[51,52] In the present work, it was found that, indeed, a significant fraction of 2-iodopropanol can be converted into the corresponding oxametallacycle. However, the chemistry of the precursor proved to be quite rich, involving additional 2-hydroxyethyl and vinyl alcohol intermediates, and leading to the production of ethylene, ethanol, acetaldehyde, water, hydrogen, and carbon monoxide in several temperature ranges. Below we offer details on our findings regarding this chemistry.

2. Experimental Section

The experiments reported here were conducted in an ultrahigh vacuum (UHV) apparatus described in detail in previous publications.[43,53,54] Briefly, this chamber is evacuated by a turbomolecular pump to a base pressure of less than 1×10^{-10} Torr and equipped with instrumentation for thermal programmed desorption (TPD), X-ray photoelectron spectroscopy (XPS), ion scattering spectroscopy (ISS), secondary ion mass spectrometry (SIMS), and Auger electron spectroscopy (AES).

TPD data were obtained by simultaneously recording up to 15 masses in a single experiment using a computer-interfaced mass spectrometer. The quadrupole mass spectrometer used for these TPD experiments is capable of detecting masses in the 1−800 amu range, and has its ionizer located inside an enclosed compartment with 7 mm diameter apertures in its front and back for gas sampling and exit to the quadrupole rods, respectively. The sample is positioned within 1 mm of the front aperture in order to detect the molecules that desorb from the front face of the crystal selectively. Because the cracking patterns for most of the gases that desorb in this system are quite complex, the raw TPD traces for each mass contain signal contributions from more than one compound; the mass spectra of all of the possible products, obtained using the same instrumental conditions, were therefore deconvoluted from the data in Figures 2 and 4.[43,55] The TPD signals are reported in arbitrary units, but their intensities are referred to the same standard given by the scale bars shown at the top of each panel of Figure 2, and calibrated to monolayers following a protocol reported previously in Figure 3.[39,56] A linear heating rate of 10 K/s was used in these TPD runs, as set by a homemade temperature controller.

XPS spectra were taken using a hemispherical electron energy analyzer set at a constant pass energy of 50 eV, which in our instrument corresponds to a resolution of about 1.2 eV full-width-at-half-maximum, and an aluminum anode. The Cu $2p_{3/2}$ at 932.7 eV, Ni $2p_{3/2}$ at 852.65 eV, and Ni $3p_{3/2}$ at 66.2 eV peaks were used for calibration of the energy scale.

The Ni(100) crystal was cut and polished using standard procedures, and spot-welded to two tantalum rods attached to a manipulator capable of cooling to liquid-nitrogen temperatures and resistively heating to above 1300 K. The crystal temperature was monitored with a chromel−alumel thermocouple spot-welded to the edge of the crystal. Cleaning of the surface by cycles of oxygen treatment, ion sputtering, and annealing were done prior to each experiment until no impurities were detected by XPS and standard CO and/or H_2 TPD could be reproduced. 2-Iodoethanol, ethanol, iodoethane, and acetaldehyde were all obtained from Aldrich (99+%) and subjected to several freeze−pump−thaw cycles before being introduced into the vacuum chamber. Normal hydrogen (99.99%), deuterium (>99.5% isotopic purity), and oxygen (99.99%) were purchased from Matheson and used as supplied. The purity of all of the compounds was checked periodically by mass spectrometry. Gas doses are reported in Langmuirs (1 L = 10^{-6} Torr s), uncorrected for ion gauge sensitivities.

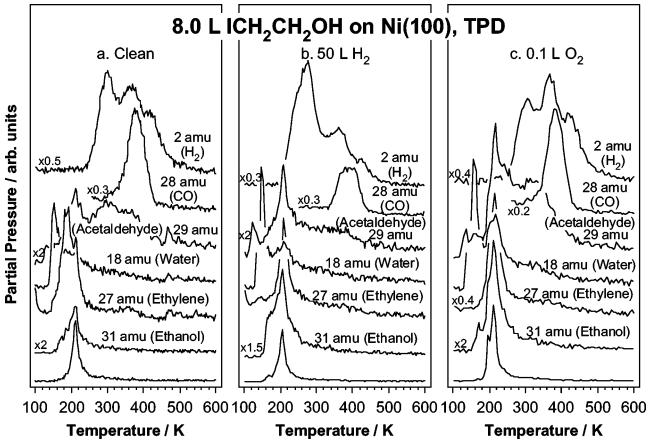

Figure 1. Temperature-programmed desorption (TPD) spectra after saturation (8.0 L) exposures of 2-iodoethanol on clean (a, left), 50 L H_2 pre-dosed (b, center), and 0.1 L O_2 pre-dosed (c, right) Ni(100) surfaces at 100 K. Heating rates of 10 K/s were used in all TPD experiments. A number of products are observed in all cases, including ethanol, ethylene, water, acetaldehyde, carbon monoxide, and hydrogen.

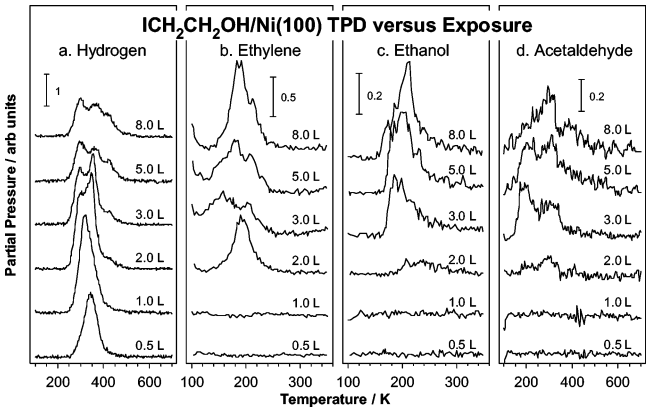

Figure 2. Hydrogen (a), ethylene (b), ethanol (c), and acetaldehyde (d) TPD spectra as a function of initial 2-iodoethanol dose on clean Ni(100) surfaces. Although complete decomposition to CO and H_2 occurs at low coverages, much more complex and stepwise chemistry is seen starting about 2 L exposures.

3. Results

The surface chemistry of 2-iodoethanol was first explored by temperature programmed desorption (TPD). Figure 1a shows TPD spectra collected after adsorption of 8.0 L of 2-iodoethanol on clean Ni(100) at 100 K. Several regimes can be identified from those data, including desorption of ethylene (27 amu) at 190 K; of acetaldehyde (29 amu), ethylene (27 amu), ethanol (31 amu), and molecular 2-iodoethanol (45 amu) at 210 K; of acetaldehyde between 250 and 400 K; and of carbon monoxide about 380 K. In addition, after peaking at 160 K, water (18

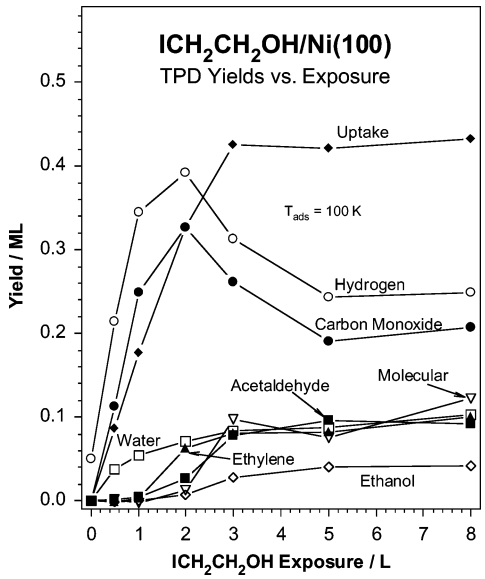

Figure 3. Hydrogen, carbon monoxide, ethylene, acetaldehyde, water, ethanol, 2-iodoethanol, and total TPD yields as a function of initial 2-iodoethanol dose on Ni(100) surfaces. The production of carbon-containing products other than CO starts about 2 L, and monolayer saturation is reached about 5 L.

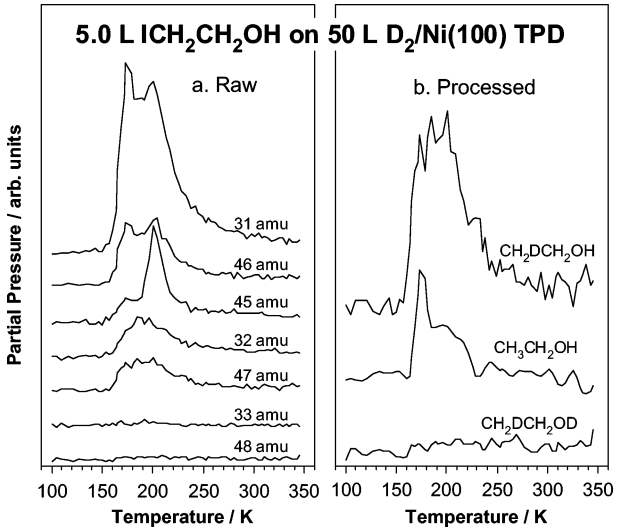

Figure 4. TPD data for 5.0 L of 2-iodoethanol adsorbed on a 50 L D_2 predosed Ni(100) surface. The left panel shows the raw traces for 31, 32, 33, 45, 46, 47, and 48 amu, whereas the right frame contains the results from deconvolution of the cracking pattern in the mass spectrometer for ethanols with different deuterium substitutions. The absence of any signal in the spectra for ethanol-d_2 argues for the formation of the alcohol via direct hydrogenation of 2-hydroxyethyl intermediates.

amu) desorption occurs continuously up to 400 K, and hydrogen desorption takes place in three main stages at about 300, 370, and 420 K. Many masses were monitored simultaneously in order to make the assignments cited above, and also to rule out desorption of other molecules such as ethylene oxide, γ-butyrolactone, carbon dioxide, or any other iodo-containing compounds. Finally, the molecular desorption seen at 210 K does not saturate with increasing exposures, indicating that it corresponds to 2-iodoethanol multilayers.

Figure 1b shows TPD spectra collected after adsorption of 8.0 L of 2-iodoethanol on a Ni(100) surface predosed with 50 L of H_2. In contrast to the case of the clean surface, most of the desorption of hydrocarbon products here is observed around 210 K: predosed hydrogen suppresses the ethylene and acetaldehyde desorption that occurs on a clean Ni(100) surface at 180 and >300 K. Moreover, ethanol production starts at lower (160 K) temperatures, and its yield increases at the expense of those for ethylene, acetaldehyde, and carbon monoxide. High-temperature (>300 K) desorption of ethylene and acetaldehyde does start at lower 2-iodoethanol exposures, 0.5 L as compared to 2.0 L on the clean surface (data not shown), but is suppressed at higher coverage. TPD spectra from 8.0 L of 2-iodoethanol adsorbed on a 0.1 L O_2 pre-dosed Ni(100) surface are presented in Figure 1c. The main changes in this case as compared to that of the clean surface are the large increases in ethylene, ethanol, acetaldehyde, CO, and molecular desorption seen around 210 K. Also, significant amounts of additional acetaldehyde desorb in a wide range of temperature above 250 K, as on the clean metal, but ethylene production at 180 K is suppressed (as with preadsorbed H_2). The high temperature states of H_2 behave in a similar fashion in all three cases.

Figure 2 displays hydrogen, ethylene, ethanol, and acetaldehyde TPD spectra for 2-iodoethanol on clean Ni(100) as a function of initial dose. These spectra were obtained by deconvolution of the cracking patterns of all products from the raw TPD data, as described in previous publications.[43,55] A peak for hydrogen desorption first grows around 350 K with increasing ICH_2CH_2OH coverage but then decreases in size and shifts to 300 K for doses above 2.0 L while a second peak develops at about 370 K; a third feature grows at about 420 K for doses over 3.0 L ICH_2CH_2OH. The ratio of the three H_2 TPD peak intensities at saturation is about 2.2:1.7:1.1, suggesting intermediates at 340 and 408 K with C_2H_3 and C_2H average stoichiometry, respectively. C_2H_4 desorption starts above 2.0 L and first peaks around 200 K, but then broadens and shifts to about 170 K at 3.0 L, growing and splitting into two peaks around 180 and 210 K at saturation. CH_3CH_2OH desorption first shows up after a 2.0 L dose as a broad feature starting about 200 K, and grows and shifts to lower temperatures with increasing initial 2-iodoethanol coverage. CH_3CHO production is initially detected between 250 and 350 K after 2.0 L ICH_2CH_2OH doses, with additional desorption developing between 150 and 250 K above 3.0 L, and a smaller third high-temperature state appearing between 350 and 450 K at saturation. Molecular ICH_2CH_2OH desorption is initially detected as a broad peak about 180 K at 3.0 L ICH_2CH_2OH that sharpens and shifts to 210 K with increasing 2-iodoethanol exposure (data not shown). Water desorption is seen in a peak that shifts from 200 K at low ICH_2CH_2OH coverages (below 1.0 L) to 180 K above 2.0 L (data not shown). Saturation in these experiments is reached after 2-iodoethanol exposures of about 5.0 L.

Desorption yields as a function of 2-iodoethanol initial dose, calculated from the ethylene, hydrogen, acetaldehyde, ethanol, 2-iodoethanol, carbon monoxide, and water TPD data discussed above after appropriate calibration,[39,56] are plotted in Figure 3. The yields for H_2 and CO production, indicative of complete decomposition, go through maxima at ICH_2CH_2OH exposures slightly above 2.0 L, but then decrease slowly at the expense of the formation of other hydrocarbon products, until reaching constant values above 5.0 L. Water desorption increases sharply with 2-iodoethanol doses between 0 and 1.0 L (the peak at 200 K), and then more slowly all the way to 8.0 L exposures (sharp desorption at 180 K). The CH_3CHO and CH_3CH_2OH yields exhibit nearly parallel behavior as a function of 2-iodoethanol coverage, both increasing sharply around 2.0−3.0 L, except that the CH_3CHO yield is always about twice that of CH_3CH_2OH. Also, it is worth noting that the CH_3CHO production is initially detected as a single broad peak around 300 K, but then develops

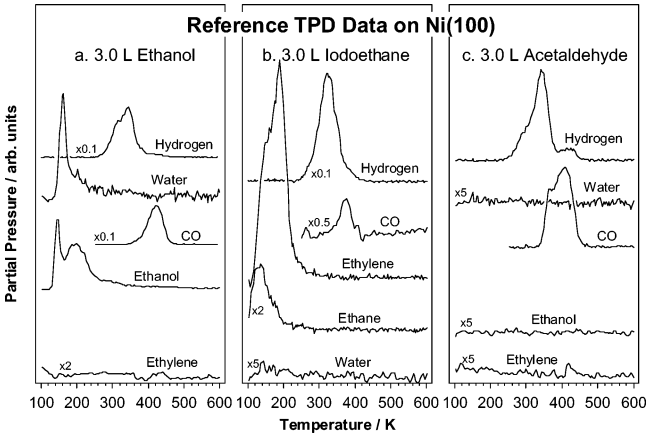

Figure 5. Reference TPD spectra for 3.0 L of ethanol (a), iodoethane (b), and acetaldehyde (c) on clean Ni(100) surfaces. The fact that virtually no acetaldehyde is produced from ethanol indicates that the acetaldehyde production from 2-iodoethanol must not involve ethanol or ethoxide intermediates. Also, the production of ethylene from iodoethane at temperatures as low as 110 K indicates the facile character of this β-hydride elimination step, and justifies our proposal of an easy conversion of 2-hydroxyethyl to vinyl alcohol. Finally, the extensive decomposition of acetaldehyde to H_2 and CO justifies the desorption of those products when starting from 2-iodoethanol.

new desorption features at about 200 and 400 K with increasing 2-iodoethanol exposures. Desorption of C_2H_4 starts at earlier coverages, after exposures of 2.0 L, but its yield then quickly levels off, and its temperature dependence also varies significantly with 2-iodoethanol coverage (see Figure 2). The onset of molecular 2-iodoethanol desorption is seen at about 3.0 L.

Figure 4 shows the TPD desorption traces recorded for the case of 5.0 L ICH_2CH_2OH adsorption on a Ni(100) surface predosed with 50 L D_2 . The left panel of that figure displays the raw TPD data for 31, 32, 33, 45, 46, 47, and 48 amu, whereas the right panel reports the results from deconvolution of those data using appropriate mass spectra cracking patterns. This deconvolution was performed in a way similar to that reported in other deuterium labeling experiments[44,57] except that mass spectra from selectively D-substituted ethanols[58] were used to determine the regioselectivity of the deuterium incorporation in our desorbing products. It is clear even from the raw data that no ethanol-d_2 at all is produced in these experiments (notice the lack of features in the 48 amu trace). This alone argues for the formation of ethanol via hydrogenation of surface 2-hydroxyethyl (eth-1-yl-2-ol) species formed by direct scission of the C−I bond in adsorbed 2-iodoethanol, without any H−D exchange on the hydroxyl moiety. The identity of the major desorbing alcohol as CH_2DCH_2OH is corroborated by the low intensity of the signal in the 32-amu trace. Some normal ethanol is also produced in these experiments, especially at low (170 K) temperatures, most likely by incorporation of normal hydrogen adsorbed from the background gases, or perhaps from some 2-iodoethanol surface decomposition. Small amounts of HD and D_2 desorption are seen above 300 K (data not shown), suggesting that there is limited incorporation of deuterium atoms and/or H−D exchange in the hydrocarbon species that form on the surface at higher temperatures.

Figure 5 shows reference TPD spectra for ethanol (a), iodoethane (b), and acetaldehyde (c), all obtained after 3.0 L exposures on clean Ni(100) at 100 K. The main desorption products from ethanol are hydrogen (at 315 and 345 K), water (160 K), and carbon monoxide (425 K), together with small amounts of acetaldehyde (in a broad feature around 300 K) and methane (300 K, data not shown); molecular desorption occurs

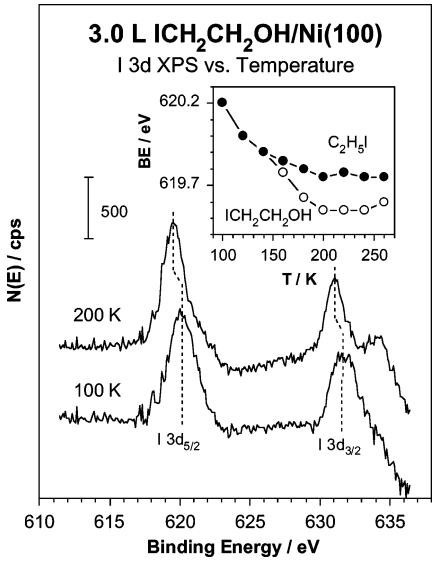

Figure 6. I 3d X-ray photoelectron spectroscopy (XPS) data for 3.0 L of 2-iodoethanol adsorbed on Ni(100) as a function of annealing temperature. The mainframe shows representative raw traces for 100 and 200 K. The inset displays the changes in the I $3d_{5/2}$ binding energy as a function of temperature for both 3.0 L of 2-iodoethanol and 3.0 L of ethyl iodide adsorbed on Ni(100). The shifts seen between 100 and 200 K are a reflection of the scission of the C−I bond in the adsorbed molecules and the formation of new hydrocarbon surface intermediates.

at about 200 (monolayer) and 150 (multilayer) K.[59] In the case of iodoethane, three main products are observed, namely, hydrogen (around 325 K), ethylene (at 150 and 190 K), and ethane (at 130 K);[60] a little methane is also produced at 340 K, but no molecular desorption is detected at this coverage. Finally, with 3.0 L of acetaldehyde on Ni(100), molecular desorption starts as early as 100 K and is supplemented by desorbing hydrogen (at 300, 345, and 430 K), carbon monoxide (365 and 410 K), and a small amount of methane (∼280 K).

The onset of the initial bond dissociation steps was identified by I 3d and O 1s XPS studies as a function of annealing temperature. I 3d XPS data were obtained for 3.0 L of both 2-iodoethanol and iodoethane adsorbed on Ni(100) at different temperatures, from 100 to 260 K in 20 K intervals. Raw data for the 100 and 200 K 2-iodoethanol cases are displayed in the main panel of Figure 6, whereas the position of the I $3d_{5/2}$ XPS peak for both compounds as a function of temperature is summarized in its inset. Neither the area nor the shape of I 3d XPS peaks are altered significantly by heating of the sample. The peak positions, however, do shift noticeably, in the case of the I $3d_{5/2}$ XPS signal for adsorbed 2-iodoethanol from 620.2 eV (molecular ICH_2CH_2OH) at low temperatures (100 K) to 619.6 eV (atomic iodine) above 160 K. This shift takes place around 150 K, and is associated with the dissociation of the C−I bond in 2-iodoethanol and the formation of 2-hydroxyethyl and atomic iodine surface species. Similar C−I bond scission kinetics is seen for iodoethane, only that in that case the I $3d_{5/2}$ XPS peak shifts down only to about 619.8 eV.

Figure 7 shows typical O 1s XPS spectra for 3.0 L of 2-iodoethanol adsorbed on clean Ni(100) as a function of adsorption temperature. A more complex behavior is seen in this case, with an overall energy shift of the maxima of the XPS feature by about 1.5 eV, from 532.7 eV at 100 K to 531.2 eV at 200 K. Quantitative information was extracted from these O 1s XPS data by fitting the raw spectra to appropriate Gaussian peaks after background subtraction. The peak fit was performed collectively by fixing most of the peak positions and peak widths

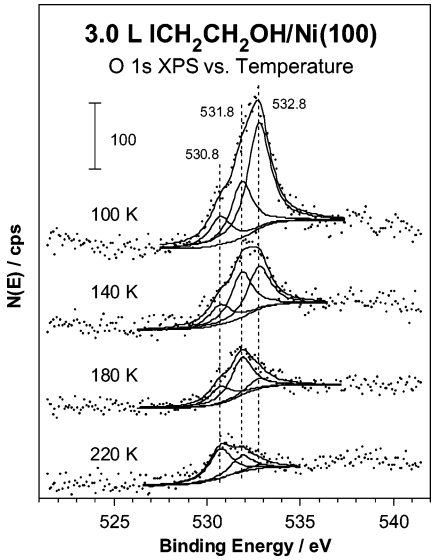

Figure 7. O 1s XPS spectra for 3.0 L of 2-iodoethanol adsorbed on Ni(100) as function of adsorbed temperature. Both the raw data and the results from fits to three Gaussian peaks centered around 530.8, 531.8, and 532.8 eV binding energies are shown. The fitted peaks are associated with mono- (adsorbed atomic oxygen), di- (HO-, RO-, ROH), and tri- (R(H)O-, H_2O-) coordinated species, respectively. There is also a component at 531.3 eV at high temperatures due to adsorbed CO.

in order to minimize the number of fitting parameters, in a manner similar to that previously reported in our studies of ammonia coadsorption with oxygen on nickel surfaces.[56] Three distinct chemical states were identified, namely, a molecular adsorbed state at 532.8 eV, an ethoxide $X-CH_2CH_2O-$ species around 531.8 eV, and adsorbed atomic oxygen at about 530.8 eV. This assignment is based on similar data for oxygen, hydroxyl and water adsorbates on nickel surfaces,[61] which in fact suggests that the peaks at 532.8 and 531.8 eV may have contributions from surface water and OH groups, respectively. Moreover, the exact identity of the ethoxide species, CH_3CH_2O-, ICH_2CH_2O-, or a $-CH_2CH_2O-$ oxametallacycle, could not be determined from these data.

The relative intensities of the three O 1s XPS states resulting from the fitting of the raw data for both 2-iodoethanol and ethanol adsorbed on Ni(100) are displayed as function of annealing temperature in Figure 8. These data were calibrated in terms of surface coverages by comparison with the TPD information in Figure 3. The disappearance of the adsorbed molecular species is indicated in both cases by the drop in intensity of the 532.8 eV signal seen between 100 and 150 K. In addition, the formation of ethoxide intermediates from adsorbed ethanol is evidenced by the increase of the signal at 531.8 eV between 150 and about 180 K. In fact, both the conversion of adsorbed ethanol to ethoxide between 140 and 160 K and the survival of the latter species to up to 260 K have been reported previously.[59] However, a more subtle change is seen with 2-iodoethanol, where the first transformation is obscured by the simultaneous early desorption of other species with unbounded OH groups (which also show up in the 531.8 eV peak in the O 1s XPS data, see below). In any case, both 2-iodoethanol and ethanol decompose further above 200 K to produce surface CO: independent experiments with CO adsorbed on clean Ni(100) indicate an O 1s XPS binding energy of 531.3 eV, the value seen above 200 K in the raw data in Figure 7.

Intensity data from O 1s XPS spectra for 2-iodoethanol on Ni(100) at 100 K as a function of initial exposure are provided

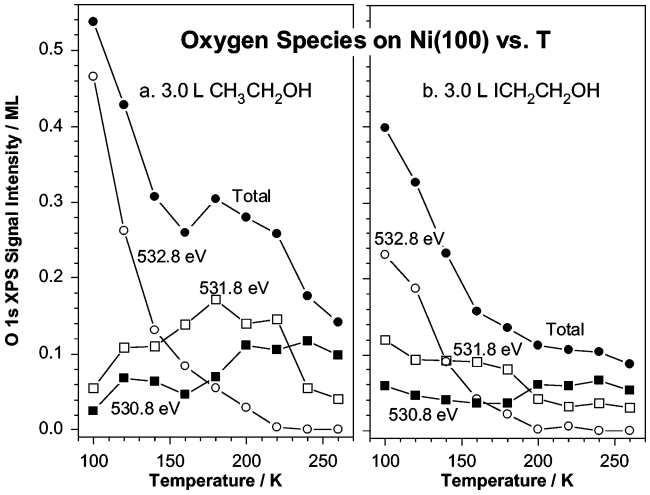

Figure 8. O 1s XPS peak areas vs annealing temperature for 3.0 L of ethanol (a) and 2-iodoethanol (b) adsorbed on Ni(100). The intensities for the three components identified by the fit shown in Figure 7 at 530.8, 531.8, and 532.8 eV binding energies are shown, all expressed in units of monolayers after appropriate calibration. The data for the 2-iodoethanol case indicate two modes of adsorption at low temperatures, with bonding through both I and O ends and via the iodine atom alone. Comparison between the ethanol and 2-iodoethanol systems also suggests a loss of the hydroxyl hydrogen around 160 K in both cases.

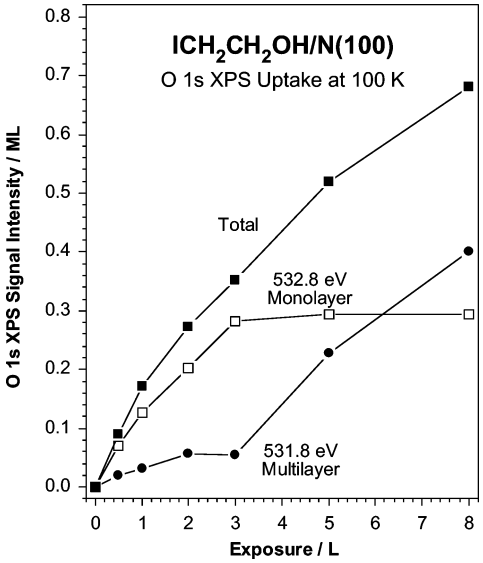

Figure 9. O 1s XPS peak areas for 2-iodoethanol adsorbed on Ni(100) as a function of initial exposure at 100 K. Again, the evolution of the different fitted peaks is displayed. In this case, the signal at 532.8 eV is associated with the main $-O(H)CH_2CH_2I-$ molecular adsorption configuration, whereas the 531.8 eV peak contains contributions from monolayer adsorbates bonded exclusively through the iodine atom and the multilayer condensation seen above 3.0 L exposures.

in Figure 9. Oxygen chemical states similar to those in Figure 7 were identified in this case as well. However, here they may represent different surface species. Note that in this uptake there is an almost linear increase in the 532.8 eV signal with coverage up to 3.0 L exposures, after which that peak levels off and the 531.8 eV feature starts to grow. This suggests that the latter peak is due to multilayer condensation, to 2-iodoethanol with hydroxyl groups away from (not interacting with) the surface. The signal at 531.8 eV is then likely to be associated with monolayer adsorption with direct bonding of the oxygen atom to the Ni(100). This interpretation can be crudely rationalized by identifying the O 1s XPS peaks at 530.8 eV with monocoordinated oxygen (oxygen bonded only to the surface), the

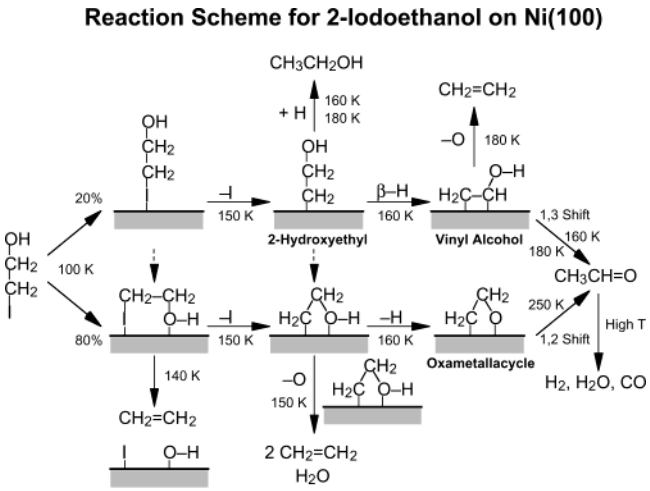

Figure 10. Overall proposed reaction scheme for the decomposition of 2-iodoethanol on Ni(100) surfaces.

features at 531.8 eV with di-coordinated species (surface hydroxide or ethoxide, or unbound alcohols), and the signals at 532.8 eV with tri-coordinated O (adsorbed water or alcohols). It does make sense for the O 1s XPS binding energy to increase with coordination, especially to the surface, because the donation of electrons from an oxygen lone pair to the metal reduces the shielding of the 1s orbital from the nucleus. A similar trend has also been recently reported for 2-propanol on Ni(100).[8,62] Based on this assignment, it can be concluded that the initial adsorption of 2-iodoethanol takes place predominantly via both hydroxyl (532.8 eV in Figure 8) and iodine (Figure 6) ends. Notice, however, that there is a small amount (about 20%, up to ~0.05 ML) of species with unbound OH groups even at low coverages (the signal at 532.8 eV). This is important because it justifies the production of ethanol via 2-hydroxyethyl intermediates in the TPD experiments (more on this later). In any case, the onset of the steep increase of the 532.8 eV signal with exposure that accompanies the saturation of the 531.8 eV peak also correlates with the start of molecular desorption.

4. Discussion

As part of our effort to elucidate the elementary surface reaction steps associated with the partial oxidation of hydrocarbons and alcohols, here we analyze the results reported above from our work on the thermal chemistry of 2-iodoethanol on Ni(100) single-crystal surfaces. A reaction network is provided in Figure 10 to guide that discussion. We first turn our attention to the adsorption mode of 2-iodoethanol on Ni(100) surfaces. On one hand, work function, photoelectron spectroscopy, and vibrational studies have indicated that low-temperature molecular adsorption of alkyl halides on metal surfaces is through the halide atom.[63,64] On the other, it has also been determined that alcohols easily bind to metals through their oxygen atom.[59,65,66] This offers several possibilities for the adsorption mode of 2-iodoethanol on metal surfaces. Our I 3d XPS data in Figure 6 clearly indicate a strong interaction between the iodine end of all adsorbed molecules and the Ni(100) substrate. However, the O 1s XPS results reported in Figures 7 and 8 point to two types of adsorption. Accordingly, we propose that approximately 80% of the 2-iodoethanol that adsorbs on Ni(100) does so through both iodine and oxygen atoms, forming a five-membered cyclic molecular intermediate ($-O(H)CH_2CH_2I-$). The remaining 20% is believed to interact only via the iodine end of the molecule, and to most likely adopt a near-perpendicular adsorption geometry with the hydroxyl group pointing away from the surface.[67,68] The I 3d and O 1s XPS data also suggest that both of these intermediates retain their molecular composition at 100 K.

Thermal decomposition of 2-iodoethanol on Ni(100) starts at quite low temperatures. Indeed, the TPD data in Figure 1 shows an onset for water desorption below 140 K. Moreover, Figure 2 indicates that at intermediate coverages ethylene production starts at temperatures as low as 120 K. These products are likely to originate from direct decomposition of molecularly adsorbed 2-iodoethanol. Low-temperature ethylene formation may occur by direct simultaneous scission of both C−I and C−O bonds in the initial $-O(H)CH_2CH_2I-$ intermediate. Both water and ethylene production around 150 K could be the result of a disproportionation reaction between two contiguous 2-iodoethanol adsorbates. Wu et al. suggested that low-temperature water formation from 2-iodoethanol on Ag(111) may not even involve the surface,[52] but the extensive isotope scrambling seen in the desorbing water when deuterium is preadsorbed (data not shown) rules that possibility in our Ni(100) system out. On the other hand, water formation by disproportionation of surface hydroxide (OH) groups only occurs at higher temperatures,[69,70] so direct water formation from 2-iodoethanol decomposition must be involved at these low temperatures. The low-temperature reaction channels proposed here are indicated schematically in the lower left corner of Figure 10.

The I 3d XPS data in Figure 6 clearly indicate that the bulk of the adsorbed species undergo a C−I bond scission step around 150 K. Indeed, the initial shifts in I 3d XPS binding energy seen there are comparable to those previously reported during the thermal activation of ethyl iodide[60] and other alkyl halides[43,45,64,71] on Ni(100). This most likely leads to the formation of two new intermediates on the surface, a majority cyclic $-O(H)CH_2CH_2-$ species (after iodine removal from $-O(H)CH_2CH_2I-$), and a small amount of 2-hydroxyethyl (eth-1-yl-2-ol) moieties. Note that we propose that C−I bond scission precedes the breaking of the O−H bond. Some of the arguments in favor of this hypothesis, such as the mechanism by which ethanol is eventually produced, are presented in the next few paragraphs. In addition, there is some precedent for such chemistry in the organometallic literature: the formation of $[Pt(CH_2CH_2OH)Cl_5]^{2-}$ by oxidative addition of 2-iodoethanol to $[PtCl_4]^{2-}$, for instance, takes place through an initial C−I bond activation.[72] Reports on Ag(111)[52,73] and Rh(111)[74] have also argued for this C−I and O−H bond-breaking sequence. In fact, it is quite possible for some of the $-O(H)CH_2CH_2-$ cyclic intermediates to form via a 2-hydroxyethyl intermediate, in particular if the lack of room on the surface at saturation forces the 2-iodoethanol into an initial upright position (with bonding through the iodine atom), and if only after the desorption of some products there is room for the oxygen atoms to interact with the nickel surface. On the other hand, the O 1s XPS uptake data do indicate a majority of oxygen-bonded species at low temperatures (as mentioned above). In any case, neither of the two resulting intermediates, the $-O(H)CH_2CH_2-$ or the 2-hydroxyethyl species, is very stable, and both react further almost immediately after their formation.

Most of the 2-hydroxyethyl intermediates undergo a reductive elimination step with atomic surface hydrogen (a hydrogenation reaction) to yield ethanol. This ethanol desorbs in two stages in the TPD spectra in Figures 1 and 2, the onsets of which are seen around approximately 160 and 180 K, respectively. The TPD data obtained on deuterium-predosed surfaces, Figure 4, clearly indicate that all of the desorbing ethanol results from

incorporation of only one hydrogen atom into the surface intermediates produced by 2-iodoethanol activation: no ethanol-d_2 at all was detected in that case. In fact, no 2-iodoethanol-d_1 formation was detected either, a result that strongly supports the claim that the C−I bond breaking step precedes the O−H bond scission (as stated above). The production of ethanol starts above 2.0 L exposures, and its yield only reaches a maximum at approximately 0.04 monolayers (1 ML = 1 molecule per surface Ni atom), less than 10% of the total adsorbed species. The identification of two desorption regimes could be accounted for by a reaction limited by the supply of hydrogen surface atoms, which may originate from different reactions at different temperatures. However, although the preadsorption of hydrogen (Figure 1) or deuterium (Figure 4) on the surface enhances the ethanol production yield, the two desorption stages still persist in those cases. We ascribe this behavior to a potential change in adsorption geometry and/or coverage as the temperature of the surface is ramped and other reactions lead to desorption of some of the adsorbed species.

The two main ethanol desorption regimes, starting around 160 and 180 K and peaking about 175 and 210 K, are accompanied by the simultaneous production of acetaldehyde. It could therefore be argued that both species may originate from the same surface intermediate, 2-hydroxyethyl. One way the production of acetaldehyde may happen is via β-hydride elimination to chemisorbed vinyl alcohol (Figure 10). Hydride elimination from the β position of adsorbed alkyls is a facile reaction that takes place at very low temperatures,[75] starting at 100 K in the case of ethyl groups on Ni(100) (Figure 5). The vinyl alcohol (an enol) can then tautomerize either on the surface or in the gas phase to form acetaldehyde. It should be noted, however, that the kinetics of acetaldehyde and ethanol production are significantly different: the acetaldehyde production seen at 160 K starts at lower coverages (2.0 L exposures) than ethanol (3.0 L) and typically shows an earlier onset in the TPD spectra, 10−20 K lower that those for ethanol. This may be a reflection of a change in selectivity between the β-hydride and reductive elimination steps as a function of coverage and temperature. It is also tempting to associate the small production of ethylene and water that starts around 200 K and peaks about 210 K to decomposition of the surface enol.

Next we discuss the thermal chemistry of the $-O(H)CH_2-CH_2-$ intermediate. Like in the case of the 2-hydroxyethyl groups, this moiety undergoes a dehydrogenation step soon after its formation, a hydrogen elimination from the hydroxyl group to yield the corresponding $-OCH_2CH_2-$ oxametallacycle. The best evidence for this dehydrogenation step, proposed to take place around 160 K, comes from the temperature dependence of the O 1s XPS data shown in Figures 7 and 8. Unfortunately, two competing phenomena seem to take place around that temperature, the dehydrogenation of $-O(H)CH_2CH_2-$ to $-OCH_2-CH_2-$ (the step proposed here) and the hydrogenation of 2-hydroxyethyl to ethanol (discussed above). The two compensate each other as far as the intensity of the 531.8 eV peak in the O 1s XPS data is concerned, so no significant changes in that feature are seen in Figure 8 between 120 and 180 K. Nevertheless, there is independent evidence available for the desorption of about 0.04 ML of ethanol in that temperature range (presented above), so the formation of a similar amount of the oxametallacycle could account for the invariance of the O 1s XPS signal. There is also a large drop in the 532.8 eV O 1s XPS peak intensity between 140 and 160 K, clearly due, at least in part, to the consumption of the $-O(H)CH_2CH_2-$ surface species. Finally, dehydrogenation of the hydroxyl group in ethanol adsorbed on Ni(100), a somewhat similar case, has been reported to occur between 140 and 160 K.[59] Oxametallacycle formation from adsorbed 2-iodoethanol has already been reported on Rh(111),[74] Ag(110),[51] and Ag(111)[52,73] single-crystal surfaces.

Last, we propose that the $-OCH_2CH_2-$ surface oxametallacycle decomposes via a 1,2 hydrogen shift in a wide temperature range above 250 K to produce additional acetaldehyde. Justification for the viability of this mechanism comes in part from recent DFT theoretical calculations on silver clusters.[76] An additional channel, involving hydrogenation of the terminal methylene of the oxametallacycle to produce surface ethoxide species, is also possible. However, only a small amount of acetaldehyde is produced when starting with ethanol, an excellent precursor for surface ethoxide, on clean Ni(100) (Figure 5), and no ethanol-d_2 was ever observed in our experiments with preadsorbed deuterium. Therefore, acetaldehyde production via hydrogenation of the oxametallacycle followed by β-hydride elimination can only be a minority pathway in this system. A β-hydride elimination to an allylic intermediate followed by hydrogenation to acetaldehyde, in analogy with the chemistry reported for platinacyclobutane on Pt(111),[39,44] can also be ruled out, because the high-temperature acetylene production is inhibited by coadsorbed hydrogen (Figure 1). Total decomposition of acetaldehyde to CO and hydrogen can easily explain the H_2 and CO high-temperature peaks (compare the appropriate traces in Figures 1 and 5). Again, the overall reaction scheme proposed in this report is summarized in Figure 10.

It is interesting to compare the reactivity of 2-iodoethanol reported here on Ni(100) to that previously seen on silver[51,52] and rhodium[74] crystals. Silver surfaces are usually less reactive than nickel substrates, a fact manifested in this case by the higher temperatures at which the thermal chemistry of 2-iodoethanol starts on the former metal. Indeed, the desorption of water, ethylene, and acetaldehyde peaks around 260 K on both Ag(110)[51] and Ag(111),[52,73] at more than 50 K higher temperatures than on Ni(100). Some sensitivity to the structure of the surface is also evident by the slight differences observed between the two silver planes studied, in particular the production of more ethanol on Ag(110) (but at higher temperatures), and the detection of a dimerization product, γ-butyrolactone, on Ag(110) but not on Ag(111). This latter product was searched for but not found in our experiments on Ni(100) either. Nevertheless, a number of general observations are common to the silver and nickel surfaces. For one, there seems to be a low-temperature reaction channel on all three surfaces that produces ethylene and water via a bimolecular step. We suggest that this disproportionation may involve initial hydrogen bonding between the hydroxyl moieties in the alcohols to facilitate the formation of H_2O; this type of interaction certainly plays a significant role in the surface chemistry of water,[69] ammonia,[56,77] and other acids on metal surfaces. Second, the thermal decomposition of 2-iodoethanol on both Ag and Ni metal surfaces appears to always be initiated by C−I bond dissociation, a step that often leads to the production of some ethanol. Third, acetaldehyde is produced in several stages, most likely through different mechanisms. Evidence has been provided in all of these studies for the eventual formation of an oxametallacycle surface species, one of the likely intermediates for high-temperature acetaldehyde production. Finally, it is worth noticing that, although the studies on silver have been motivated by the desire to understand the catalytic epoxidation of olefins, no ethylene

oxide production has yet been detected in any of the systems investigated to date.

The reactivity of 2-iodoethanol on rhodium is quite unique, despite its lesser activity in catalysis than nickel and its intermediate position in the periodic table between Ag and Ni. In particular, surface-science studies on rhodium single crystals have pointed to an easy decarbonylation of primary alcohols, presumably via the formation of oxametallacycle intermediates similar to those cited here.[5,6] During the thermal activation of 2-iodoethanol on Rh(111), only hydrogen, carbon monoxide, and methane are seen to desorb from the surface.[74] The decarbonylation reaction is still proposed to occur via acetaldehyde formation, only that the subsequent decomposition of that product appears to dominate over its molecular desorption. The authors of that study suggested a mechanism involving 2-hydroxyethyl and vinyl alcohol intermediates, in line with the ideas put forward to explain the chemistry on silver and nickel. The β-hydride elimination step from 2-hydroxyethyl to a coordinated vinyl alcohol is also central in the Wacker process, which uses a palladium complex to convert alkenes to aldehydes.[78] In the final analysis, it seems that most late transition metals promote the same fundamental elementary steps during the conversion of halo alcohols, hydroxyalkyls, and oxametallacycles, and that the differences in selectivity in the catalytic behavior of the different metals is due to subtle changes in the relative rates of the competing reactions.[3,7]

Our interest in studying the surface chemistry of 2-iodoethanol on Ni(100) arose from the broader goal of understanding the mechanistic parameters that control selectivity in partial oxidation reactions. More specifically, we focus on the conversion of alcohols in oxidation environments. The balance between dehydrogenation and dehydration of organic alcohols provides a classical example of the importance of controlling selectivity in catalysis: whereas acidic oxides such as γ-alumina are in general active in dehydration to olefins, basic oxides such as magnesia and calcium oxide promote dehydrogenation to aldehydes and ketones instead.[22] Moreover, the surface reactivity of alcohols is closely connected to that of alkyl groups in oxygen-treated substrates, because the latter are believed to dissociatively adsorb to form surface alkyls[79] and then undergo oxygen insertion and form the same alkoxides intermediates seen after initial dehydrogenation of adsorbed alcohols.[11,13]

Dehydrogenation of alcohols to aldehydes or ketones has been reported over a number of late transition-metal surfaces.[50,80,81] Isotope labeling experiments have clearly demonstrated that this reaction occurs via direct $\beta-$H elimination of alkoxide surface species,[8,23] in analogy to the easy β-hydride elimination that takes place on adsorbed alkyls species.[48,75,82] In contrast, alcohol dehydration has been observed on some early transition metals.[23] It is still not clear what the sequence of steps may be in the dehydration reactions, where C−O bond scission may precede, follow, or occur simultaneously with $\gamma-$H elimination.[83] The case has been made for early hydrogen elimination on Mo(110),[84] but no conclusive evidence for this is yet available, and more systematic studies are needed to settle this issue. In nonacidic solids, $\beta-$H elimination is expected to dominate over $\gamma-$H elimination, but even there two key questions remain still unanswered: (1) what controls the regioselectivity of the hydrogen removal; and (2) in the case of $\gamma-$H elimination, what are the subsequent steps available to the resulting oxametallacycle intermediate. The studies reported here aimed to answer the second question. It has become clear from our work that an early $\gamma-$H elimination from adsorbed alcohols could lead to the formation of $-O(H)CH_2CH_2-$ cyclic intermediates, and that those can easily disproportionate to ethylene (and water). In other words, facilitating hydrogen removal at the γ position shifts selectivity from dehydrogenation to dehydration. On the other hand, it was also seen that oxametallacycles can also isomerize to yield aldehydes (or ketones). The key in shifting selectivity in nonacidic catalyst toward dehydration may be to promote $\gamma-$H elimination before the removal of the hydroxyl hydrogen from the alcohol. Preliminary work in our laboratory with 1,1,1-trifluoro-2-propanol has provided evidence for the possibility to switch selectivity from β- toward γ-hydride elimination in alkoxides by inductive effects.[85] Future studies will address this issue in more detail.

5. Conclusions

I 3d and O 1s XPS data indicate that 2-iodoethanol adsorbs molecularly on clean Ni(100) at 100 K by adopting two possible geometries, a majority $-O(H)CH_2CH_2I-$ species anchored to the surface through both the iodine and oxygen atoms, and a minority configuration attached only via the iodine end of the molecule. The initial activation of those two species occurs around 150 K, and involves the scission of the C−I bond to yield $-O(H)CH_2CH_2-$ and 2-hydroxyethyl intermediates, respectively. A low-temperature decomposition channel does seem to precede that reaction, producing small amounts of ethylene and water starting around 140 K. This pathway most likely involves either the simultaneous breaking of both C−I and C−O bonds in the $-O(H)CH_2CH_2I-$ molecular species and/or a disproportionation between two interacting (hydrogen-bonded) $-O(H)CH_2CH_2-$ surface moieties once the C−I bond has been broken.

The 2-hydroxyethyl intermediate resulting from iodine removal in iodine-bonded molecular species reacts further starting at around 160 K via two competing steps, a reductive elimination with surface hydrogen to produce ethanol and a β-hydride elimination to yield surface vinyl alcohol. Ethanol desorption is indeed seen in TPD experiments, in two peaks with maxima around 175 and 210 K, and its origin from hydrogenation of 2-hydroxyethyl intermediates is corroborated by the incorporation of only one deuterium atom when D_2 is predosed on the Ni(100) surface. On the other hand, the vinyl alcohol converts further on the surface, a small amount loosing its oxygen atom to produce ethylene (detected around 210 K) and the rest tautomerizing to acetaldehyde (at 180 and 210 K in TPD experiments).

Based on O 1s XPS data as a function of temperature, it is proposed that the $-O(H)CH_2CH_2I-$ intermediate dehydrogenates around 160 K to produce a $-OCH_2CH_2I-$ surface oxametallacycle. This intermediate has previously been identified on silver single-crystal surfaces, and proposed on rhodium, palladium, and other transition metals. At higher temperatures, that oxametallacycle isomerizes via a 1,2 hydrogen shift to yield acetaldehyde, some of which desorbs in a wide temperature range starting around 250 K and peaking about 300 K. Hydrogenation of the oxametallacycle to ethoxide can be ruled out by the absence of significant production of acetaldehyde from adsorbed ethanol (a good precursor for the ethoxide species), and also by the absence of any ethanol-d_2 production in experiments with coadsorbed 2-iodoethanol and deuterium. Formation of acetaldehyde via a β-hydride elimination of oxametallacycle to an allylic species followed by rehydrogenation at the terminal methylene moiety is also discarded based on the inhibition of high-temperature acetaldehyde production in the presence of surface hydrogen. Finally, high-temperature H_2 and CO desorption may be accounted by decomposition of

adsorbed acetaldehyde, because similar chemistry is observed when starting from that adsorbate.

Acknowledgment. Financial support for this research was provided by the Department of Energy, Basic Energy Sciences Division, under Contract DE-FG03-01ER15182.

References and Notes

(1) Martino, G. In *12th International Congress on Catalysis (Studies in Surface Science and Catalisis Series, Vol. 130)*; Corma, A., Melo, F. V., Mendioroz, S., Fierro, J. L. G., Eds.; Elsevier: Amsterdam, 2000; p 83.
(2) Thomas, J. M.; Thomas, W. J. *Introduction to the Principles of Heterogeneous Catalysis*; Academic Press: London, 1967.
(3) Zaera, F. *J. Phys. Chem. B* **2002**, *106*, 4043.
(4) Haber, J. In *Handbook of Heterogeneous Catalysis*; Ertl, G., Knözinger, H., Weitkamp, J., Eds.; VCH: Weinheim, Germany, 1997; Vol. 5, p 2253.
(5) Mavrikakis, M.; Barteau, M. A. *J. Mol. Catal. A* **1998**, *131*, 135.
(6) Madix, R. J.; Roberts, J. T. In *Surface Reactions (Springer Series in Surface Sciences, Vol. 34)*; Madix, R. J., Ed.; Springer-Verlag: Berlin, 1994; p 5.
(7) Zaera, F. *Acc. Chem. Res.* **2002**, *35*, 129.
(8) Gleason, N. R.; Zaera, F. *J. Catal.* **1997**, *169*, 365.
(9) Gleason, N. R.; Zaera, F. In *3rd World Congress on Oxidation Catalysis, San Diego, California, 21−26 September 1997 (Studies in Surface Science and Catalysis Series, Vol. 110)*; Grasselli, R. K., Oyama, S. T., Gaffney, A. M., Lyons, J. E., Eds.; Elsevier: Amsterdam, 1997; p 235.
(10) Zaera, F.; Gleason, N. R.; Klingenberg, B.; Ali, A. H. *J. Mol. Catal. A* **1999**, *146*, 13.
(11) Zaera, F.; Guevremont, J. M.; Gleason, N. R. *J. Phys. Chem. B* **2001**, *105*, 2257.
(12) Ali, A. H.; Zaera, F. *J. Mol. Catal. A* **2002**, *177*, 215.
(13) Zaera, F. *Catal. Today* **2002**, *81*, 149.
(14) Collman, J. P.; Hegedus, L. S.; Norton, J. R.; Finke, R. G. *Principles and Applications of Organotransition Metal Chemistry*; University Science Books: Mill Valley, CA, 1987.
(15) Jørgensen, K. A.; Schiøtt, B. *Chem. Rev.* **1990**, *90*, 1483.
(16) Lambert, R. M.; Ormerod, R. M.; Tysoe, W. T. *Langmuir* **1994**, *10*, 730.
(17) Calhorda, M. J.; Lopes, P. E. M.; Friend, C. M. *J. Mol. Catal. A* **1995**, *97*, 157.
(18) Shekhar, R.; Barteau, M. A.; Plank, R. V.; Vohs, J. M. *Surf. Sci.* **1997**, *384*, L815.
(19) Sachtler, W. M. H.; Backx, C.; van Santen, R. A. *Catal. Rev., Sci. Eng.* **1981**, *23*, 127.
(20) Campbell, C. T.; Paffett, M. T. *Surf. Sci.* **1984**, *139*, 396.
(21) Serafin, J. G.; Liu, A. C.; Seyedmonir, S. R. *J. Mol. Catal. A* **1998**, *131*, 157.
(22) Cimino, A.; Stone, F. S. In *Handbook of Heterogeneous Catalysis*; Ertl, G., Knözinger, H., Weitkamp, J., Eds.; VCH: Weinheim, Germany, 1997; p 845.
(23) Wiegand, B. C.; Uvdal, P.; Serafin, J. G.; Friend, C. M. *J. Phys. Chem.* **1992**, *96*, 5063.
(24) March, J. *Advanced Organic Chemistry: Reactions, Mechanisms, and Structure*; McGraw-Hill: Tokyo, 1968.
(25) Pines, H. *The Chemistry of Catalytic Hydrocarbon Conversions*; Academic Press: New York, 1981.
(26) Zaera, F. *Acc. Chem. Res.* **1992**, *25*, 260.
(27) Tjandra, S.; Zaera, F. *J. Vac. Sci. Technol.* **1992**, *A10*, 404.
(28) Lin, J.-L.; Bent, B. E. *J. Phys. Chem.* **1992**, *96*, 8529.
(29) Tjandra, S.; Zaera, F. *J. Catal.* **1993**, *144*, 361.
(30) Solymosi, F. *Catal. Today* **1996**, *28*, 193.
(31) Janssens, T. V. W.; Zaera, F. *J. Phys. Chem.* **1996**, *100*, 14118.
(32) Wu, G.; Kaltchev, M.; Tysoe, W. T. *Surf. Rev. Lett.* **1999**, *6*, 13.
(33) Janssens, T. V. W.; Zaera, F. *J. Catal.* **2002**, *208*, 345.
(34) Liu, Z.-M.; Zhou, X.-L.; Buchanan, D. A.; Kiss, J.; White, J. M. *J. Am. Chem. Soc.* **1992**, *114*, 2031.
(35) Zaera, F.; Bernstein, N. *J. Am. Chem. Soc.* **1994**, *116*, 4881.
(36) Tjandra, S.; Zaera, F. *J. Catal.* **1996**, *164*, 82.
(37) Ihm, H.; White, J. M. *Langmuir* **1998**, *14*, 1398.
(38) Celio, H.; Smith, K. C.; White, J. M. *J. Am. Chem. Soc.* **1999**, *121*, 10422.
(39) Chrysostomou, D.; Zaera, F. *J. Phys. Chem. B* **2001**, *105*, 1003.
(40) Zaera, F.; Tjandra, S.; Janssens, T. V. W. *Langmuir* **1998**, *14*, 1320.
(41) Scoggins, T. B.; White, J. M. *J. Phys. Chem. B* **1999**, *103*, 9663.
(42) Tjandra, S.; Zaera, F. *J. Phys. Chem. B* **1997**, *101*, 1006.
(43) Tjandra, S.; Zaera, F. *J. Phys. Chem. A* **1999**, *103*, 2312.
(44) Chrysostomou, D.; Chou, A.; Zaera, F. *J. Phys. Chem. B* **2001**, *105*, 5968.
(45) Tjandra, S.; Zaera, F. *J. Am. Chem. Soc.* **1995**, *117*, 9749.
(46) Zaera, F. *Isr. J. Chem.* **1998**, *38*, 293.
(47) Zaera, F. *Prog. Surf. Sci.* **2001**, *69*, 1.
(48) Zaera, F. *Appl. Catal.* **2002**, *229*, 75.
(49) Madix, R. J. *Acc. Chem. Res.* **1979**, *12*, 265.
(50) Weldon, M. K.; Friend, C. M. *Chem. Rev.* **1996**, *96*, 1391.
(51) Jones, G. S.; Mavrikakis, M.; Barteau, M. A.; Vohs, J. M. *J. Am. Chem. Soc.* **1998**, *120*, 3196.
(52) Wu, G.; Stacchiola, D.; Kaltchev, M.; Tysoe, W. T. *Surf. Sci.* **2000**, *463*, 81.
(53) Zaera, F. *Surf. Sci.* **1989**, *219*, 453.
(54) Gleason, N. R.; Zaera, F. *Surf. Sci.* **1997**, *385*, 294.
(55) Chrysostomou, D.; French, C.; Zaera, F. *Catal. Lett.* **2000**, *69*, 117.
(56) Guo, H.; Chrysostomou, D.; Flowers, J.; Zaera, F. *J. Phys. Chem. B* **2003**, *107*, 502.
(57) Janssens, T. V. W.; Zaera, F. *Surf. Sci.* **2002**, *501*, 16.
(58) Burr, J. G. *J. Phys. Chem.* **1957**, *61*, 1477.
(59) Kratochwil, T.; Wittmann, M.; Kuppers, J. *J. Electron Spectrosc. Relat. Phenom.* **1993**, *64−5*, 609.
(60) Tjandra, S.; Zaera, F. *Surf. Sci.* **1993**, *289*, 255.
(61) de Jesús, J. C.; Carrazza, J.; Pereira, P.; Zaera, F. *Surf. Sci.* **1998**, *397*, 34.
(62) Gleason, N.; Guevremont, J.; Zaera, F. *J. Phys. Chem. B* **2003**, submitted.
(63) Zhou, Y.; Henderson, M. A.; Feng, W. M.; White, J. M. *Surf. Sci.* **1989**, *224*, 386.
(64) Tjandra, S.; Zaera, F. *Langmuir* **1992**, *8*, 2090.
(65) Sexton, B. A.; Rendulic, K. D.; Hughes, A. E. *Surf. Sci.* **1982**, *121*, 181.
(66) Davis, J. L.; Barteau, M. A. *Surf. Sci.* **1990**, *235*, 235.
(67) Zaera, F.; Hoffmann, H.; Griffiths, P. R. *J. Electron Spectrosc. Relat. Phenom.* **1990**, *54/55*, 705.
(68) Jenks, C. J.; Bent, B. E.; Bernstein, N.; Zaera, F. *J. Phys. Chem. B* **2000**, *104*, 3008.
(69) Guo, H.; Zaera, F. *Catal. Lett.* **2003**, in press.
(70) Backstrand, K. M.; Weibel, M. A.; Moision, R. M.; Curtiss, T. J. *J. Chem. Phys.* **2000**, *112*, 7209.
(71) Tjandra, S.; Zaera, F. *Langmuir* **1994**, *10*, 2640.
(72) Luinstra, G. A.; Wang, L.; Stahl, S. S.; Labinger, J. A.; Bercaw, J. E. *J. Organomet. Chem.* **1995**, *504*, 75.
(73) Linic, S.; Medlin, J. W.; Barteau, M. A. *Langmuir* **2002**, *18*, 5197.
(74) Brown, N. F.; Barteau, M. A. *J. Phys. Chem.* **1994**, *98*, 12737.
(75) Zaera, F. *J. Am. Chem. Soc.* **1989**, *111*, 8744.
(76) Linic, S.; Barteau, M. A. *J. Am. Chem. Soc.* **2003**, *125*, 4034.
(77) Guo, H.; Zaera, F. *Surf. Sci.* **2003**, *524*, 1.
(78) Parshall, G. W.; Ittel, S. D. *Homogeneous Catalysis: The Applications and Chemistry of Catalysis by Soluble Transition Metal Complexes;* 2nd ed.; Wiley: New York, 1992.
(79) Benziger, J. B.; Madix, R. J. *J. Catal.* **1980**, *65*, 36.
(80) Xu, X.; Friend, C. M. *Surf. Sci.* **1992**, *260*, 14.
(81) Shekhar, R.; Barteau, M. A. *Catal. Lett.* **1995**, *31*, 221.
(82) Zaera, F. *Chem. Rev.* **1995**, *95*, 2651.
(83) Kraus, M. In *Handbook of Heterogeneous Catalysis*; Ertl, G., Knözinger, H., Weitkamp, J., Eds.; VCH: Weinheim, Germany, 1997; p 1051.
(84) Wiegand, B. C.; Uvdal, P. E.; Serafin, J. G.; Friend, C. M. *J. Am. Chem. Soc.* **1991**, *113*, 6686.
(85) Zhao, Q.; Zaera, F. *J. Am. Chem. Soc.* **2003**, in press.